Impact of Smart Transformer Voltage and Frequency Support in a high renewable penetration system

Junru Chen*[1], Muyang Liu[1], Giovanni De Carne[2], Rongwu Zhu[3], Marco Liserre[3], Federico Milano[1], and Terence O'Donnell[1]
1. University College Dublin
2. Karlsruhe Institute of Technology
3. Kiel University

Abstract

Increasing penetration of power electronics interfaced generation decreases the stability of the system, due to the absence of the rotational inertia in their operation. Emulation of the inertia using converter controls in combination with storages can address this issue. However, this method relies on the use of large quantities of storage to compensate power during a transient power unbalance. Instead of increasing the supply, the smart transformer (ST), with fast response, offers the possibility to dynamically regulate the demand. This paper investigates the use of an ST to dynamically control reactive power and demand to support voltage and frequency respectively in the grid. The demand is controlled dynamically to emulate inertia. From an analysis based on a 250 kVA, 10kV/400V LV distribution network, it is shown that a demand variation in the range of 6-10% can be achieved. These results are extended to a case study based on the entire all-Island Irish Transmission system which shows that widespread use of STs with these controls could potentially facilitate a 10% increase in wind penetration without the inclusion of any other storage.

Keywords—Smart Transformer, Inertia Emulation, Frequency Support, Voltage Support, High Wind Penetration.

1 Introduction

The European Commission targets a 40% cut in greenhouse gas emissions compared to 1990 levels and at least a 27% share of renewable energy consumption in

*Corresponding author, email: Junru.chen.1@ucdconnect.ie

2030 [1]. Many countries with high renewable penetration, such as Denmark, have a considerable exchange capacity with their neighbouring power systems. This strong interconnection facilitates export of power during overproduction and import of power in case of incidents such as massive disconnection of renewables [2]. On the other hand, other countries such as Ireland, which recently announced a target of 70% of electricity from renewable generation, have a very limited interconnection capacity to its neighbours. For example, Ireland is only interconnected with Northern Ireland via a 1320 MW double circuit tie line and with the United Kingdom via a 500 MW HVDC link [2]. Under such situations, the system must carry significant reserves from conventional generators, from interruptible load and pumped storage hydroelectricity, in order to reduce the frequency variation and prevent the frequency collapse following the contingency [3]. However, with increasing renewable generation, conventional generation may become economically unviable and displaced from the system. Furthermore, power electronics-interfaced renewables, such as wind turbines and PV plants, offer no rotational inertia to the system. This leads to the increase in the rate of change of frequency (RoCoF) that may trigger frequency relays and consequently cause the automatic under-frequency load shedding. This has led to many investigations into alternative sources for flexibility and frequency support in low inertia power systems such as the use of storage and demand response. At a practical level, for example, to provide a financial incentive for the provision of flexibility, the Irish system operator has introduced a range of new system services, such as synchronous inertia and fast frequency response in order to counteract potential issues with frequency stability[4].

Significant attention has also been given to the provision of virtual inertia from converter interfaced generation. This can be achieved by providing an extra power component proportional to the rate of change of frequency (RoCoF). The required energy can be provided either from the rotational inertia of the wind turbine [5], de-rated operation of the renewable generation [6], or from co-located electric energy storage system (ESS) [7]. Such approaches have been implemented in wind farms

[8,9], PV systems [10] and electric vehicle charging stations [11]. Obtaining the inertial support from the rotational inertia of the wind turbine implies a recovery period after the contingency where the turbines track back to their maximum power point. De-rated operation of the renewable generation implies a financial cost to the power plant operator. Use of co-located storage to supply the frequency support may require the provision of large quantities of ESS. On the other hand, as back-up regulation to the primary frequency control, contracted load shedding or demand response schemes can be employed and, for example, the Irish system experiences 2.8 such events on average per year [12].

As an alternative approach to the load shedding, frequency support can be provided from the demand by acting on voltage-dependent loads. Following a voltage variation, these loads change their power demand, and thus they can represent a controllable resource for providing frequency support in the system. The concept of varying the load consumption by acting on the voltage is not new. Conservation Voltage Reduction (CVR) [13] has already been used in distribution grids for energy saving purposes. Implemented via transformer tap changers, the load demand can be reduced during the peak time for avoiding congestion. However, due to the slow action of the mechanical tap, CVR dynamics are limited. Another application of this concept is based on the use of a Static Var Compensator (SVC) to vary the demand voltage [14]. In this method, to support the frequency, the voltage should typically be reduced after the contingency. However, if a grid voltage dip occurs along with the contingency then the SVC main function of compensating reactive power to maintain the voltage may conflict with a frequency support function. In this paper a Smart Transformer (ST) is used to provide the voltage variation. In contrast to the SVC, the ST can perform coordinated and simultaneous voltage and frequency support [15], since its voltage regulation on the primary and secondary side are fully independent.

The ST [16], a power electronics-based transformer [17,18], increases grid controllability, providing grid services without the need for additional hardware [16].

The main advantage of the ST is that the voltage and reactive power regulation in its primary and secondary side are decoupled. Using this advantage, the ST, in the primary side can independently compensate the reactive power to the transmission system in order to support the grid voltage. In the secondary side, ST can identify the voltage and frequency sensitivity and then control the demand [19], providing services: reverse power flow control [20], soft load reduction [21], and real time primary frequency regulation [22-24]. The dynamic control (response time less than 100 ms) of the demand consumption [26] is much faster than the conventional CVR applications, which not only support the frequency but also improve the transiently stability with respect to the inertia provision [15]. The device-level analysis of this function has been well researched in terms of the control design and application [15, 19, 22, 23], and the effects of the ST stability in response to the variable frequency [24]. However, from the system level point of view, whether this control can really improve the system stability or how much the system stability can be improved with the respect to the penetration of the ST in the grid is still unknown and needs to be answered before a massive application of the ST.

Although the ST is well discussed in device level, the study about its impact on the dynamic behavior and stability of the overall power system is lacked. The contribution of this paper is, therefore, to quantify the improvement of the system stability, in terms of the frequency stability, voltage stability and transient stability with respect to the ST in the system of different renewable penetrations. The availability of a demand reduction and reactive power compensation is firstly quantified via a common residential distribution system in Manchester, UK. The system stability is quantified via a case study in the Irish system with different renewable penetration.

The paper is structured as follows: Section II reviews the ST topology and its frequency and voltage support functions. Section III analyses the frequency support obtained by application of the ST in a 250 kVA, 400 V distribution network. Section IV provides the simulation results when applied in the all-island Irish transmission

system and quantifies the improvement from the control on the system wind penetration, while section V draws the conclusions.

2 Smart Transformer Flexible Demand Control

The common configuration of the ST is a 3-stage topology consisting of an MV AC/DC rectifier, MVDC/LVDC converter with a high frequency transformer and LVDC/LCAC inverter as shown in Fig.1. Besides the MVAC and LVAC ports corresponding to the primary and secondary side of the traditional transformer, this ST topology also has MVDC and LVDC ports, which provide capability to connect renewable generators, electric vehicle chargers and energy storage system. The MV AC/DC converter connects to the utility grid, uses a PLL to achieve synchronization and applies the conventional decoupled power control to maintain the MVDC voltage. The MVDC/LVDC converter regulates the LVDC voltage, controlling the power flow between two DC links. The LV DC/AC converter supplies the ST-fed grid, controlling the voltage amplitude and frequency. The freedom on the voltage regulation and electric isolation between each ports provide the ability of the independent voltage and reactive power control in each port. Consequently, the voltage in the LVAC side can be controlled to vary the demand in a range in response to the frequency and the reactive power in the MVAC side can be controlled to support the voltage, so that the system stability can be improved. This section reviews these functions.

2.1 Load Voltage Sensitivity Identification

The objective of the flexible demand control is to regulate the demand depending on the power system frequency, i.e. reduce the demand in under-frequency situation while increase the demand in over-frequency situation, through load voltage control. To achieve the desired loading power control, the load voltage sensitivity is used to identify the load active power sensitivity to voltage, as described in [19]. Considering an exponential load representation (1), the power is dependent on the voltage as:

$$P_L = P_{L0}\left(\frac{V_{L0}}{V_{L0}}\right)^n \quad (1)$$

where PL,0 is the active power demand at nominal voltage VL0, the exponential value n is the load voltage coefficient, P_L is the active power demand at a certain rms voltage VL.

The voltage sensitivity S_V, defined as the percentage of power reduction ΔP_L resulting from a percentage of voltage reduction ΔV_L as in (2), is used to detect the load voltage coefficient n in (1).

$$S_V = \frac{\Delta P_L}{\Delta V_L} \approx n \tag{2}$$

When the ST applies the load identification procedure, it purposely applies a 1% trapezoidal voltage disturbance in its LVAC output, measures the power and computes (2) at specified time instants during the voltage variation [21]. It should be noted that the sensitivity identification procedure is independent from the adopted load model, but an exponential model has been adopted due to its simplicity in representing the load response to voltage variations. The load identification step shall be performed anytime that it is deemed necessary (e.g. in response to a significant loading variation), depending on the variability of the identified load. It must be noted that the applied voltage disturbance is small enough that it does not impact on the grid voltage quality.

2.2 ST Frequency support

This section introduces the basic frequency support control [15], which varies the demand following a grid frequency deviation. As shown in (2), if $S_V > 0$, it means demand reduction will result from a voltage reduction, otherwise $S_V < 0$ means that a demand reduction will results from a voltage increase. Based on this feature, the demand consumption can be shaped to emulate the conventional generators inertial behavior. The available power to support frequency can be determined as:

$$\begin{cases} \Delta P_{L,Vmax} = S_V \dfrac{V_L^* - V_{Lmax}}{V_L^*} \\ \Delta P_{L,Vmin} = S_V \dfrac{V_L^* - V_{Lmin}}{V_L^*} \end{cases} \tag{3}$$

where V_{Lmax}/V_{Lmin} is the maximum/minimum ST inverter output voltage. To be noted, that the load voltage shall be limited within the range, e.g., $(V_L^* \pm 0.1)\ pu$, according to EN 50160 [27], where V_L^* is the voltage nominal value.

The classical swing equation is represented in (4), where M is the inertia and D is the turbine governor gain.

$$P_g = M\Delta\dot{\omega}_g + D\Delta\omega_g + P_L \tag{4}$$

In order to mimic the behavior of (4), the flexible demand control based on the voltage and power relationship (3) is proposed in (5). The control links the MV grid frequency, detected by the PLL, to the ST inverter output voltage V_L^{*r}. The gain K_t is used to change the inverter voltage according to the RoCoF $\Delta\dot{\omega}_g$, while the droop gain K_d is used to change the voltage proportionally to the frequency deviation $\Delta\omega_g$. Finally, the frequency droop and RoCoF terms sum up to determine the ST inverter output voltage reference V_L^{*r}:

$$V_L^{*r} = \frac{-S_V}{|S_V|}\left(K_t\Delta\dot{\omega}_g + K_d \cdot \Delta\omega_g\right) + V_L^* \tag{5}$$

where $K_t\Delta\dot{\omega}_g + K_d \cdot \Delta\omega_g$ is the controlled ST inverter voltage variation, $\frac{-S_V}{|S_V|}$ is the relationship (positive or negative) between the voltage change and demand change. Combing (2),(3),and (5), the conventional swing equation (6) is obtained, where $S_V P_{L0} K_t$ is the virtual inertia and $S_V P_{L0} K_d$ is the droop gain in system level. Note, the minus sign in (6) indicates that the demand should decrease in the under-frequency situation.

$$P_L = -S_V P_{L0} K_t \Delta\dot{\omega}_g - S_V P_{L0} K_d \cdot \Delta\omega_g + P_{L0} \tag{6}$$

It can be seen that from (6), that the emulated inertia depends on the load voltage sensitivity S_V, loading level P_{L0} and RoCoF gain K_t. The load voltage sensitivity S_V is

related to the type of the load, i.e. the residential load voltage sensitivity is 1.2~1.5, the commercial load is 0.99~1.3, and industrial load is 0.18 [28]. Apparently, applying such control to the residential and commercial loads has more benefit than applying it to the industrial load. The loading level P_{L0} is the system demand controlled by the ST. It can be concluded that increasing the number of ST-connected residential and commercial loads can potentially improve the system transient and frequency stability.

For the frequency support, in Ireland, the grid code [29] commands that controlled devices, e.g. distributed generators, shall attempt to maximize/minimize active power, when the frequency goes outside the 50±2 Hz, and shall be able to ride through RoCoF of 1.0 Hz/s [30]. Meanwhile, the load voltage variation shall be within ±0.1 pu [27]. Considering these, the ST inverter output voltage should be controlled to the limits ±0.1 pu when either the frequency deviation is 2 Hz (0.04 pu) or the RoCoF is 1.0 Hz/s (0.02 pu/s). Thus, here we suggest $K_d = 0.1\ (pu)/0.04\ (pu) = 2.5$ and $K_t = 0.1\ (pu)/0.02\ (pu/s) = 5$. It should be noted that the grid code [28] stipulates also the control dead-bands which for $\Delta\omega_g$ is 0.2 Hz, and for $\Delta\dot{\omega}_g$ is 0.02 Hz/s.

2.3 ST Voltage support

Beside the supply of active power, the ST can use the remaining power capacity $Q_{ST,max}$, to inject reactive power for supporting the MV grid voltage. In this respect the ST behaves like a STATCOM [31], with the application of a similar control strategy, i.e. voltage-to-reactive power droop control as in (7).

$$Q_{ST} = K_q\left(V_M^* - V_{M,d}\right) + Q_0 \tag{7}$$

$$Q_{ST,max} = \sqrt{S_{ST}^2 - P_L^2} \tag{8}$$

where K_q is the voltage-to-reactive power droop gain, Q_0 is the initial reactive power injection, $K_q\left(V_M^* - V_{M,d}\right)$ is the additional reactive power injection, V_M^* is the MV side nominal voltage, and Q_{ST} is the ST total reactive power output to MV grid. The ST

priority is delivery of active power P_L to the load (6), thus, the reactive power compensation is limited according to (8), i.e. $-Q_{ST,max} \leq Q_{ST} \leq Q_{ST,max}$.

For the voltage support, the grid code in Ireland commands that the power factor shall be 0.95 leading to lagging, when local voltage deviation is less than 0.1 pu [32]. Thus, K_q should be selected according to (9) based on the consideration of a maximum 0.95 power factor for the extreme voltage variation, i.e. 0.1 pu.

$$0.1K_q \leq \sqrt{1-0.95^2}P_{L0} - Q_0 \tag{9}$$

2.4 Discussion

Equations (2~9) construct the flexible demand control as shown in Fig. 1. Hence, by dynamically controlling the demand and compensating reactive power, this control can improve the system transient, frequency and voltage stability.

The flexible demand control is used to support the system stability in dynamic, which aims to move the operating point back to its set-up, but not purposely raising the voltage or lowering the demand to change the system power flow. In other words, the purpose of this control is to improve the system stability, to reduce the occasion of the loading shedding and avoid the blackout, but not change the power dispatch.

Some of the load in practice may present as a dynamic recovery load, e.g. thermostatically controlled loads, which is identified as impedance loads in a short timeframe, and as constant power loads in the longer timeframe. Typically, the recovery time of this kind of load is around 2 min [40], while the control focuses on the fast response and primary control. This recovered loading power is still be compensated by the generators via a secondary regulation. The flexible demand control purposely does not be designed to achieve zero steady state frequency and voltage error, in order to activate the secondary control of the generator and drag the system back to the nominal state, consequently the control of the ST backs to the nominal state as well. Because of above load type, this control presents to a heavy weight on the

inertia support. Also because in (6), the demand is easily approaching its minimum value at the beginning of the contingency, where both $\Delta\omega_g$ and $\Delta\dot{\omega}_g$ are considerable, i.e. frequency nadir in the first swing and large initial ROCOF. The paper emphases the quantification of the system stability improvement by the inclusion of the ST, thus, only shows the result in the time scale of the primary control and the load in the rest of the paper is modeled as exponential load.

3 Distribution System Analysis

In order to quantify the demand flexibility available from a typical distribution system, the proposed flexible demand control is applied to, a 250 kVA, 10 kV/400 V (based on an ENWL distribution network in Manchester, UK, [33]) consisting of total 90 residential customers evenly distributed across three phases, with 32, 26 and 32 customers in phase A, B and C respectively. The network is shown in Fig. 2 [34] and is divided into three areas, for the purposes of presentation of unbalanced and stochastic load data. The load is modeled as an exponential load (1) with its winter daily loading profile P_{L0} at the feeder terminal given in Fig. 3 [34]. The load data has a one-minute resolution and the system power flow for each one minute is solved by the Matlab *fsolve* function. The simulation first verifies the load voltage sensitivity identification method by purposely introducing a 1% voltage reduction and using (2) to compute the sensitivity. Based on this, it quantifies the available active and reactive power which can be used to support the grid stability from this distribution system.

Fig. 4 shows the results of the voltage sensitivity identification. The cyan line shows the result from computing the sensitivity every 1 min. However, the voltage sensitivity does not need to be computed frequently, but only needs to be re-computed when the load undergoes a significant change. Fig. 4 also shows the voltage sensitivity which results from re-computing in response to a load change ΔP of greater than 20%, 40% and 60%. The increase in computation threshold reduces the computation frequency but also reduces the precision as a trade-off. For example, when the threshold for re-computing is set at 60%, the load identification only needs to be done 7 times daily.

The proposed flexible demand control does not require a precise voltage sensitivity to be effective but only needs the sign of the S_V to avoid an adverse demand regulation, thus, a reasonable setting may be to re-compute for a 40% threshold resulting in 18 load identification steps in a day.

In the distribution system, due to the line impedance and its consequent voltage drop, the end-line load voltage is commonly the minimum voltage in the network and should not fall outside the range of 0.9 to 1.1 pu, according to the EN 50160 standard. Thus, the minimum ST inverter voltage used to support frequency in (3) should consider the end-line load voltage and should dynamically change with the loading variation. Reference [26] introduces the method to determine the minimum supply voltage linked to the loading in the distribution system. In the ST application, Fig. 5 shows the possible ST inverter voltage range for the grid under investigation. Correspondingly, Fig. 6 (a) shows the load active power variation range, and Fig. 6 (b) shows the available active power, used to support the frequency, as a percentage of the nominal situation, where “demand reduction” corresponds to the minimum voltage in under-frequency and “demand increase” corresponds to the maximum voltage in over-frequency. Since the minimum voltage is variable and greater than 0.9 pu but the maximum voltage is a constant 1.1 pu, the power (on average 6%) used to support the under-frequency situation is lower than that (on average 10%) used to support an over-frequency situation from the same distribution system.

The ST rating matches the distribution network maximum apparent power consumption i.e. 250 kVA. The active power delivery under different voltage situations is given in Fig. 6 (a), while the remaining power capacity can be used to compensate the reactive power into the utility grid for voltage support purposes, as shown in Fig. 7. It can be seen that the available reactive power is limited during peak demand time to nearly 150 kVar or 0.6 pu, and the reduction in the voltage or demand can provide more available reactive power to support voltage. This interaction is favorable with the distributed load voltage sensitivity $S_V > 0$, because a frequency reduction normally

requires a voltage reduction, so that the reduced demand P_L in (8) allows an increase in the feasible reactive power compensation $Q_{ST,max}$.

4 Case study in all-island Irish Transmission system

The previous section characterized the level of frequency and voltage support which might be available from a single distribution system. This section extrapolates this support to an entire power system to attempt to quantify the potential benefit at transmission system level. The Irish power system is considered as a case study. It should be noted that, in the following case studies, the STs work in closed loop with the main power system, where their active and reactive power demand influence the main power system voltage and frequency, and vice versa.

The Irish Transmission system grid data is provided by EirGrid, the Irish TSO, consisting of 1,479 buses, 1,851 transmission lines and transformers, and 245 loads as shown in Fig. 8. The model is built into Dome, a Python-based power system software tool [35]. There are 21 conventional synchronous power plants modeled as 6th order synchronous machine models with automatic voltage regulators and turbine governors, 6 power system stabilizers, and 176 wind power plants, of which 142 are doubly-fed induction generators and 34 direct drive wind turbines achieving 40.97% wind penetration (WP). This model provides a dynamic representation of the actual Irish electrical grid with accurate topology and load data. It should be noted that the dynamic data of generators are not the actual generator data but can reflect the real Irish system dynamics. The details of the device models are given in [36]. The consumption of electricity in Ireland is shared by 31.4% in residential, 26.9% in commercial and 39.3% in industrial loads in 2015 [37].

For the purposes of the whole system level simulation the aggregated effect of all of the MV/LV STs is represented as STs interfaced between the transmission system and the loads. Due to the lack of the DC grid in Irish system, the DC connections of the ST is neglected. The model of the ST refers to the differential-algebraic equation model in

[38] and has been validated via a comparison with the result from hardware in-the-loop [39]. The ST size or capacity is set as 100% of initial loading. The settings for the proposed flexible demand control are the ones identified in Section II. The load connected through the ST is modeled as an exponential load with voltage coefficient 1.5 for residential loads and 1.0 for commercial loads [28]. The grid frequency is measured locally in each of the ST. As a contingency in the case study, the HVDC line to the United Kingdom, which represents the largest infeed to the system, disconnects at 1 s while importing 0.4 GW. The overall system load at this time is 2.36 GW.

We investigate two cases. Case 1 considers the effect of the ST flexible demand control on the system voltage and frequency after the contingency, if the residential and/or commercial load is controlled by the ST with the flexible demand control. Case 2 and 3 quantifies frequency and voltage stability respectively under an increase in wind penetration. The aim of these cases is to quantify the extra level of non-synchronous generation allowable, from the perspective of frequency and RoCoF limits, assuming the load is ST controlled.

4.1 Case 1: Voltage/frequency control in Irish grid

In this case, we first apply the ST with flexible demand control to the residential load only, as its voltage coefficient is the highest [28], and then additionally apply the ST to the commercial load, compared with the original system with no ST. Fig. 9 shows (a) the grid frequency and (b) the bus voltage at the capital city, Dublin, after contingency.

It can be seen from Fig. 9 (a) that the proposed control can improve the system frequency response after the contingency, especially as regards RoCoF reduction. Because there is sufficient primary control from the generation, the ST control has limited benefit on the frequency deviation in this case. It can also be seen that the application of the ST to the residential loads has the largest effect with an additional smaller effect from the commercial loads, which is due to the residential loads having higher voltage coefficient and load occupation, thus contributing higher inertia as

explained in (6).

From Fig. 9 (b), it can be seen that the reactive power compensation from the ST can improve the voltage response after the contingency. It is worth noting that the voltage behavior at the instant of the contingency (1-1.5 s) for each scenario is similar, this is because the available reactive power during this period is limited due to the converter capacity limit. However, following the frequency reduction, the proposed control reduces the loading which frees converter capacity for reactive power compensation. Thus, after 1.5 s the voltage response improves.

4.2 Case 2: Frequency stability in high wind penetration

In this case, the possible maximum wind penetration while maintaining frequency stability, in the Irish system with the flexible demand control under the same contingency (loss of the HVDC line) is investigated. The Irish grid code requires that the frequency deviation shall remain within a ±2 Hz range and limits RoCoF to 1 Hz/s in the first 500 ms and 0.5 Hz/s calculated over 500 ms [30]. In order to increase the wind penetration, the SGs are gradually replaced by the direct drive WG thus also losing their frequency and voltage support functions. For each wind penetration level, simulations similar to those in Fig. 11 are performed. The frequency nadir, RoCoF in the first 500 ms and steady-state value are recorded and plotted in Fig. 10.

From Fig. 10 (a), the increase in WP reduces the frequency nadir and increases the RoCoF due to the reduction of the system inertia. The proposed control if applied on both residential and commercial load has considerable improvements on the frequency nadir. However, when the WP reaches around 85%, this improvement becomes negligible as the available frequency response is simply inadequate to compensate for the reduced system inertia. This indicates that the supports from the load aspects is limited, and the achievement for 100% WP should still rely on the renewable generator controls. As a result, in relation to limiting the frequency nadir within ±2 Hz or 48 Hz, the proposed control applied to residential load can improve the WP from 73.1% to 83.96% but applying it to the additional commercial load has only a slight

improvement, increasing from 83.96% to 84.88%. This is because the voltage sensitivity of the residential load is higher than the commercial load, and the application of the ST in the residential load can obtain the maximum benefits on the system frequency and transient stability. The additional application on the commercial load is not very appreciable compared with its expensive installation cost.

On the other hand, regarding the RoCoF limit of 1 Hz/s, the maximum WP for the no ST case is constrained to 63.49%, while in this case, the use of the proposed control can push the WP to 72.96% and 77.61% corresponding to the ST control applied to residential loads or additionally commercial loads (Fig. 12(b)).

With the replacement of SGs by wind generators, turbine governor response is being removed and hence the steady state frequency in Fig. 10 (c) is decreasing with the WP increase. The ST frequency support in the steady state is limited, up to 6% for the residential load for a 2 Hz frequency deviation, and is linked to the steady-state frequency with a droop gain. Therefore, the application of the ST can improve the steady-state frequency deviation. However, even at the highest wind penetration, the worst frequency deviation is 1 Hz, which corresponds to 3% load reduction in ST controlled load, so that the steady-state frequency improvement is very little, only 0.1 Hz, from the application of the ST.

In total, considering the nadir and RoCoF limits resulting from the loss of largest infeed, the proposed control could increase the WP by approximately 10% WP in the Irish system without the use of any additional storage. However, in order to keep the same steady state frequency, the inclusion of extra power support is required. This reflects that the inclusion of the ST with such control has more beneficial on the inertia support with respect to the RoCoF and frequency nadir improvement, rather than the frequency support.

4.3 Case 3: Voltage stability in high wind penetration

In this case, we focus on the voltage stability in the case of the increase in WP. To

investigate the impact of the reactive power compensation from the ST alone, the WG do not implement any voltage-to-reactive-power-droop control, i.e. they behave like a constant power source. Therefore, the WP increase and the associated decrease in SG AVR response results in the voltage at the Dublin bus decreasing in both nadir and the steady-state value as shown in Fig. 11.

It can be seen in Fig. 11 (a) that the application of the ST results in only a slight improvement in the voltage nadir, on average 0.005 pu, considerably less than the effect on the frequency nadir. This is because the voltage support is mainly dependent on its local reactive power compensation while the frequency support is global. This is also the reason that the voltage nadir reduces in a less consistent manner and it is dependent on the location of the replaced SG, unlike the frequency nadir which shows consistent reduction with the gradual increase in WP.

As shown in Fig. 11 (b), the steady-state voltage tendency is similar with the steady-state frequency tendency in this process. This is owing to the voltage to reactive power droop compensation in the ST. The lower the steady-state voltage, the higher the reactive power compensation, and thus, improvements from the application of the ST become significant.

5 Conclusions

The fast response ST enables the demand to be dynamically controlled in the same manner as VSM control applied to storage, to support voltage and frequency in the grid. Through the analysis and quantification of the control applied to a general distribution system in Manchester, UK and to the Irish system, it can draw following conclusions:

i) The flexible loading used to support frequency from a typical residential area is approximately 6% for an under-frequency situation, and 10% for an over-frequency situation. Meanwhile, the available reactive power capacity can be used to support

voltage, depending on the loading level but at least to 0.6 pu.

ii) The application of the ST with such control can provide a considerable inertia into the system, which can help improve 10% wind penetration without add of other inertia emulator with the same transient stability level.

iii) This control in the steady state (of primary regulation) is limited, especially the improvement on the voltage stability is poor when the loading is heavy as simulated in the paper. If the system aims to keep the same steady state response, extra power support sources are required to take the place of the TG response, and reactive power compensation from WGs is still required.

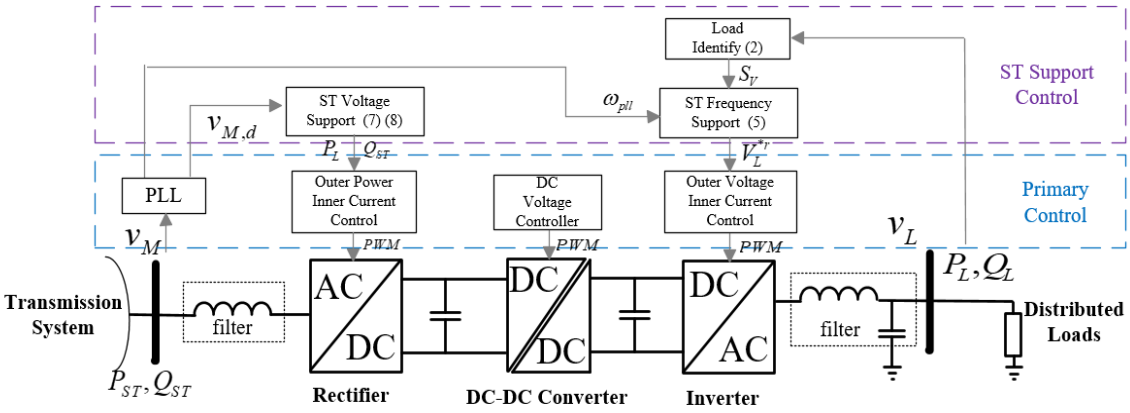

Fig.1 Smart transformer structure with system support control

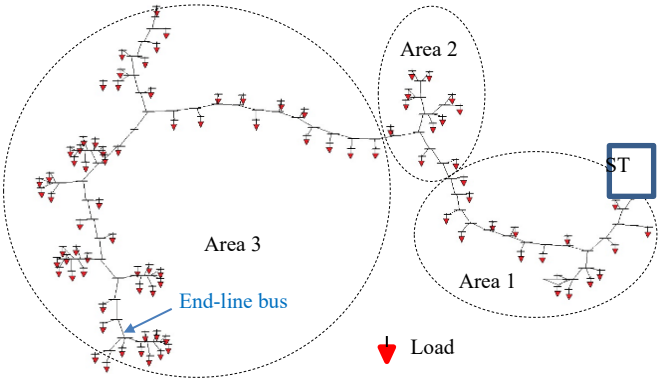

Fig. 2. ENWL distribution network in Manchester.

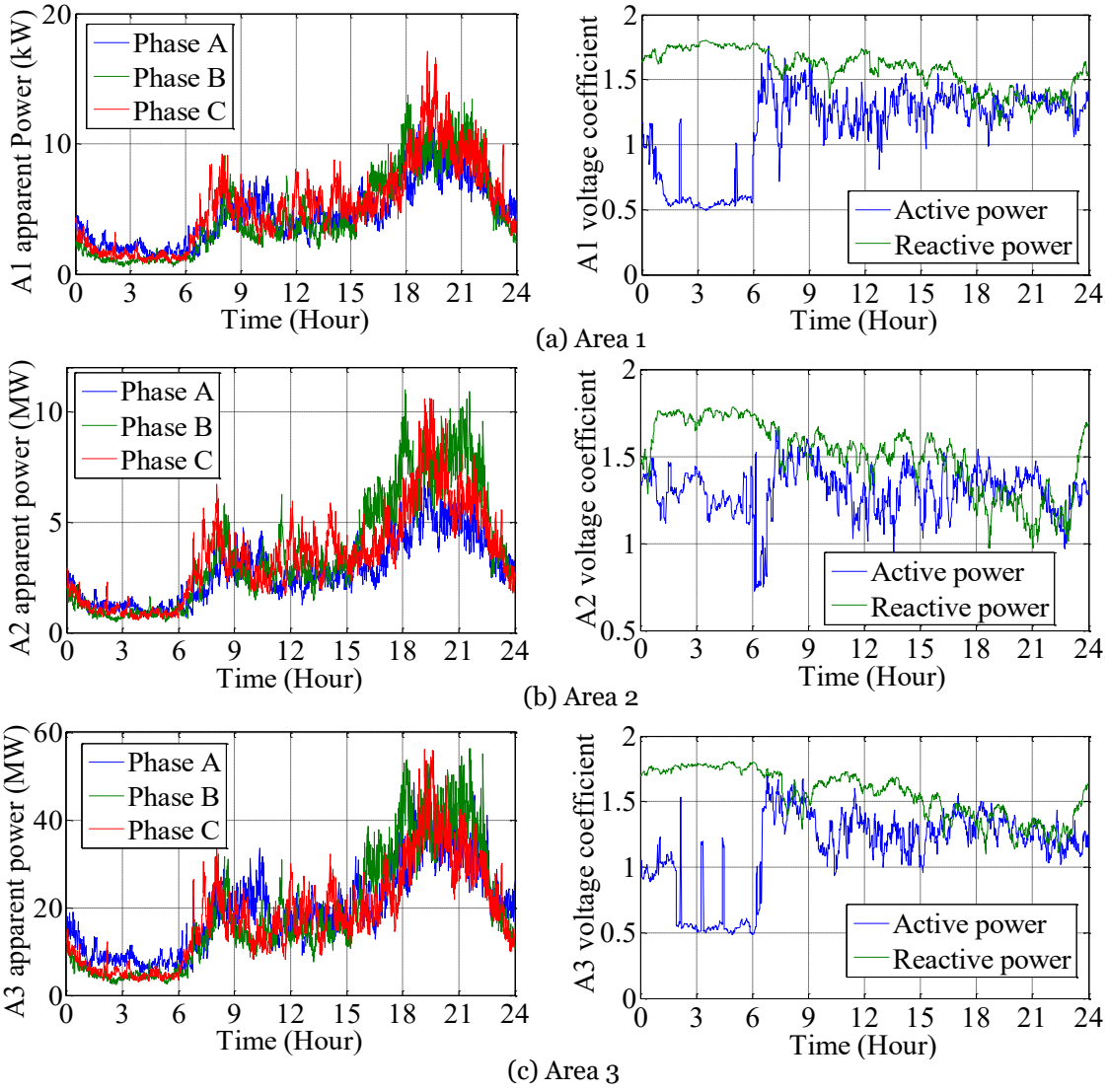

Fig. 3. Winter daily three phase loading profile in area 1, 2 and 3.

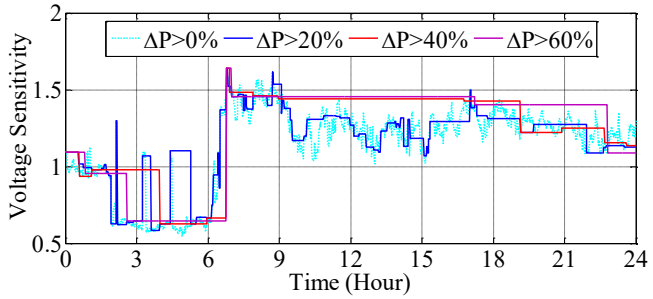

Fig. 4. Load voltage sensitivity identification of the distribution network.

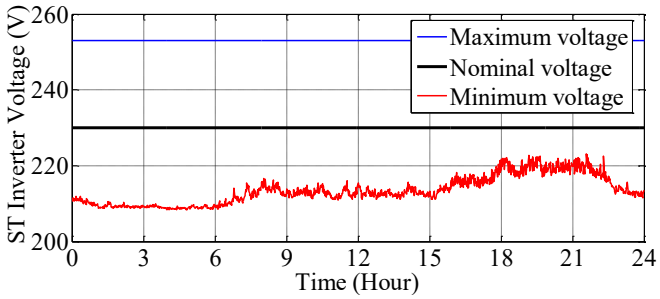

Fig. 5. Safety network supply voltage range.

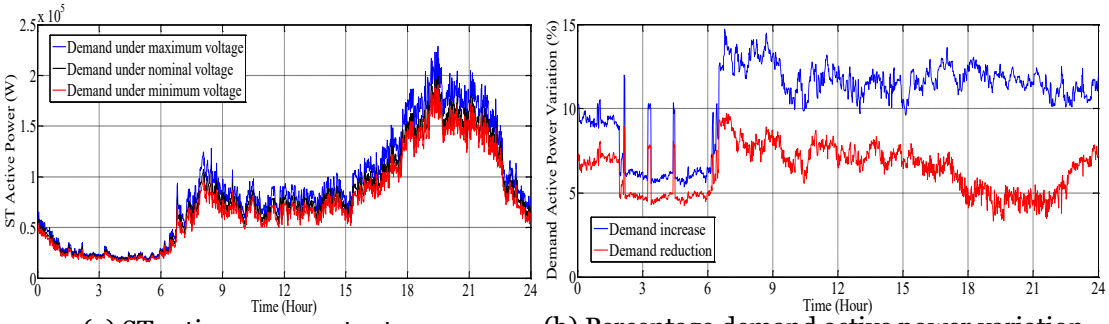

(a) ST active power output range. (b) Percentage demand active power variation.

Fig. 6. Available load active power for frequency support.

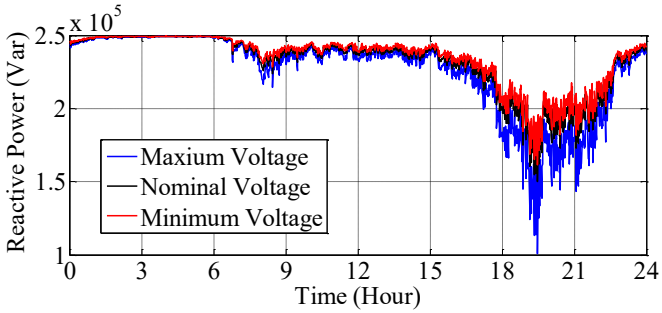

Fig. 7. Available ST reactive power for voltage support.

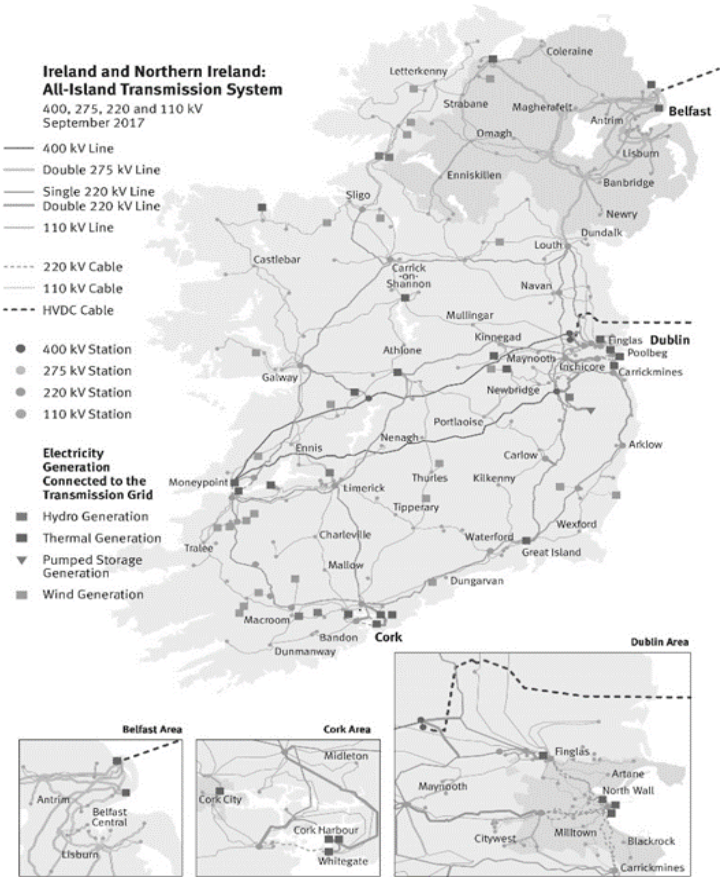

Fig. 8. All-island Irish power system map (available at: www.eirgridgroup.com).

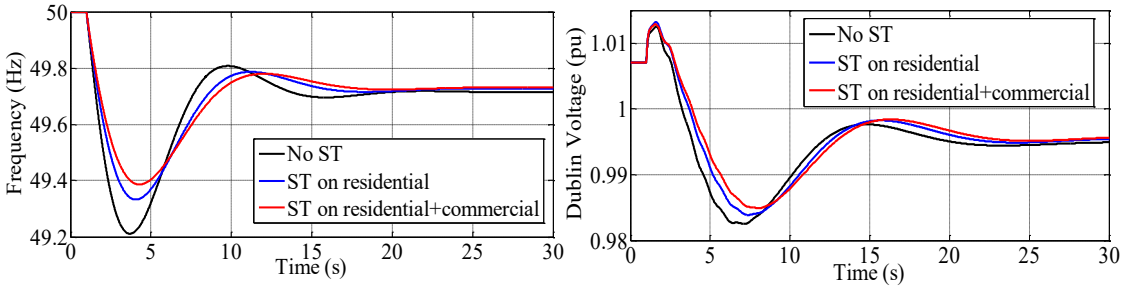

(a) Grid frequency (b) Dublin bus voltage

Fig. 9. Case 1 results.

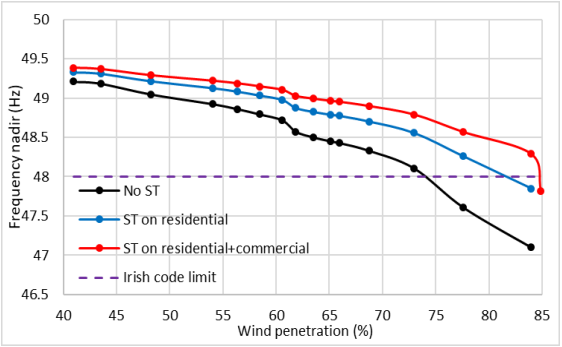

(a) Frequency nadir VS. wind penetration.

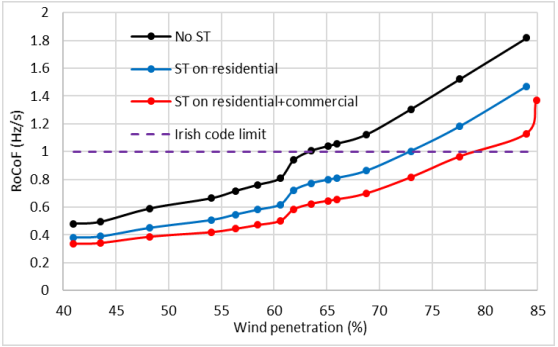

(b) RoCoF VS. wind penetration.

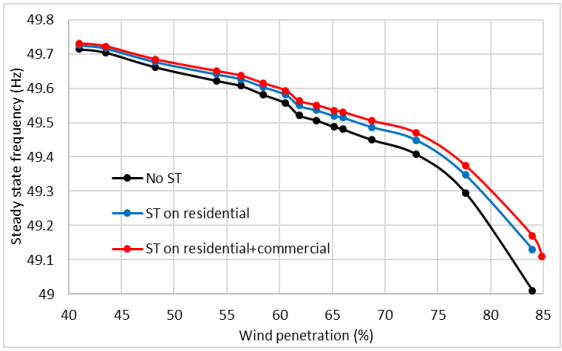

(c) Steady state frequency VS. wind penetration.

Fig. 10. Case 2 results.

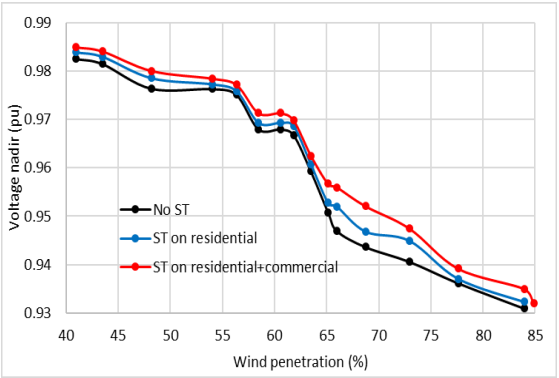

(a) Voltage nadir VS. wind penetration.

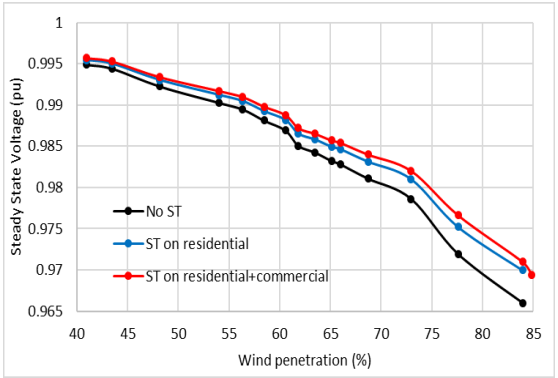

(b) Voltage nadir VS. wind penetration.

Fig. 11. Case 3 results.

Acknowledgements

This work is funded by the Science Foundation Ireland (SFI) Strategic Partnership Programme Grant Number SFI/15/SPP/E3125, SFI/15/IA/3074, the European Research Council (ERC) under grant 616344 HEART, and the Ministry of Science, Research and the Arts of the State of Baden-Wurttemberg Nr. 33-7533-30-10/67/1.

References

[1] European Commission, ” A policy framework for climate and energy in the period from 2020 to 2030” Brussels, 22, Jan. 2014.

[2] N. Aparicio, et al. “Automatic under-frequency load shedding mal-oeration in power systems with high wind power penetration,” *Elsevier*, May 23, 2016.

[3] J. Machowski, J. W. Bialek, and J.R. Bumby, “Power System Dynamics: Stability and Control,” John Wiley & Sons, Inc, second edition, 2008.

[4] EirGrid and SONI, “DS3 System Services Qualification Trials Process Outcomes and Learnings 2017,” 6 Nov. 2017.

[5] L. Zeni, A. Rudolph, J. Münster-Swendsen, I. Margaris, A. Hansen, and P. Sørensen, “Virtual inertia for variable speed wind turbines,” *Wind Energy*, vol. 16, no. 8, pp. 1225–1239, 2013.

[6] Xin, H., Liu, Y., Wang, Z., et al.: ‘A new frequency regulation strategy for photovoltaic systems without energy storage’, IEEE Trans. Sustain. Energy, 2013, 4, (4), pp. 985–993

[7] S. Arco, J. A. Suul and O. B. Fosso, "A Virtual Synchronous Machine implementation for distributed control of power converters in Smart Grids," *Electric Power Systems Research*, Vol. 122, pp. 180-197, May 2015.

[8] Y. Ma, W. Cao, L. Yang, F. Wang and L. Tolbert, “Virtual Synchronous Generator Control of Full Converter Wind Turbines With Short-Term Energy Storage”, *IEEE Trans. Ind. Electron.*, Vol. 64, no. 11, pp. 8821-8831, Nov. 2017.

[9] L. Huang et al., ”Synchronization and Frequency Regulation of DFIG-Based Wind Turbine Generators with Synchronized Control,” *IEEE Trans. Engergy Conversion*, vol. 37, no. 3, pp. 1251-1262, Spet. 2017.

[10] Q-C. Zhong, Z. Ma, W. Ming and G. C. Konstantopoulos, “Grid-friendly wind power systems based on the synchronverter technology,” *Energy Conversion and Management*, Vol. 89, 1 Jan. 2015, pp. 719-726.

[11] J. A. Suul, S. D'Arco and G. Guidi, "Virtual Synchronous Machine-Based Control of a Single-Phase Bi-Directional Battery Charger for Providing Vehicle-to-Grid Services," in *IEEE Transactions on Industry Applications*, vol. 52, no. 4, pp. 3234-3244, July-Aug. 2016.

[12] Soni and Eirgrid, “All-Island Transmission System Performance Report,” 2017.

[13] P. Sen and K. Lee,” Conservation Voltage Reduction Technique: An Application Guideline for Smart Grid,” *IEEE Tran. Ind. Appl.*, Vol. 52, No. 3, May/June 2016.

[14] Y. Wan, M. A. A. Murad, M. Liu and F. Milano, "Voltage Frequency Control Using SVC Devices Coupled With Voltage Dependent Loads," in *IEEE Transactions on Power Systems*, vol. 34, no. 2, pp. 1589-1597, March 2019.

[15] J. Chen *et al.*, "Smart Transformer for the Provision of Coordinated Voltage and Frequency Support in the Grid," IECON 2018 - 44th Annual Conference of the IEEE Industrial Electronics Society, Washington, DC, 2018, pp. 5574-5579.

[16] L. Ferreira Costa, G. De Carne, G. Buticchi and M. Liserre, "The Smart Transformer: A solid-state transformer tailored to provide ancillary services to the distribution grid," *IEEE Power Electron. Mag.*, vol. 4, no. 2, pp. 56-67, June 2017.

[17] A. Q. Huang, M. L. Crow, G. T. Heydt, J. P. Zheng, and S. J. Dale, “The future renewable electric energy delivery and management (FREEDM) system: The energy internet,” *Proc. IEEE*, vol. 99, no. 1, pp. 133–148, Jan. 2011.

[18] X. She, X. Yu, F. Wang and A. Q. Huang, "Design and Demonstration of a 3.6-kV–120-V/10-kVA Solid-State Transformer for Smart Grid Application," *IEEE Trans. Power Electron.*, vol. 29, no. 8, pp.3982-3996, Aug. 2014.

[19] G. D. Carne, M. Liserre, and C. Vournas, “On-line load sensitivity identification in lv distribution grids,” *IEEE Tran. Power Sys.*, vol. 32, no. 2, pp. 1570–1571, March 2017.

[20] G. De Carne, G. Buticchi, Z. Zou and M. Liserre, "Reverse Power Flow Control in a ST-Fed Distribution Grid," *IEEE Trans. Smart Grid*, vol. 9, no. 4, pp. 3811-3819, July 2018.

[21] G. De Carne, G. Buticchi, M. Liserre and C. Vournas, “Load Control Using Sensitivity Identification by means of Smart Transformer,” *IEEE Tran.Smart Grid*, Vol. P, no. 99, Oct. 3, 2016.

[22] G. De Carne, G. Buticchi, M. Liserre and C. Vournas, "Real-Time Primary Frequency Regulation using Load Power Control by Smart Transformers," *IEEE Trans.Smart Grid, Early Access*.
[23] J. Chen, R. Zhu, T. O'Donnell and M. Liserre, "Smart Transformer and Low Frequency Transformer Comparison on Power Delivery Characteristics in the Power System," 2018 AEIT International Annual Conference, Bari, 2018, pp. 1-6.
[24] Z. Zou, G. De Carne, G. Buticchi and M. Liserre, "Smart Transformer-Fed Variable Frequency Distribution Grid," in *IEEE Transactions on Industrial Electronics*, vol. 65, no. 1, pp. 749-759, Jan. 2018.
[25] D. G. Shah, D, M. L. Crow, "Online Volt-Var Control for Distribution Systems With Solid State Transformers," *IEEE Trans. Power Del*, vol. 31, no. 1, pp 343 – 350, Feb. 2016.
[26] J Chen; C O'Loughlin; T O'Donnell, "Dynamic demand minimization using a smart transformer", Proc. 43rd Annual Conference of the IEEE Industrial Electronics Society, IECON 2017, Beijing, China, Dec. 2017, pp 4253 – 4259.
[27] Copper Development Association "Voltage Disturbances Standard EN 50160- Voltage Characteristics in Public Distribution Systems", July 2004, Power Quality Application Guide.
[28] Electric Power Research Institute, "Measurement-Based Load Modelling," CA: 2006. 1014402.
[29] EirGrid, "EirGrid Grid Code Version 6.0," 22 July 2015.
[30] EirGrid and SONI, "RoCoF Alternative & Complementary Solution Project, Phase 2 Study Report," 31 March, 2016.
[31] X. Gao, G. De Carne, M. Liserre and C. Vournas, "Voltage control by means of smart transformer in medium voltage feeder with distribution generation," Power Tech, 2017 IEEE Manchester, 20 Jul. 2017.
[32] ESB Networks, "The Distribution System Security and Planning Standards," Jan. 2015.
[33] I. Ibrahim, V. Rigoni, C. Loughlin, S, Jasmin and T. Donnell, "Real- time Simulation Platform for Evaluation of Frequency Support from Distributed Demand Response," Cigre Symposium Dublin 2017.
[34] J. Chen, T. Yang, C. Loughlin and T. M. O'Donnell, "Neutral Current Minimization Control for Solid State Transformers under Unbalanced Loads in Distribution Systems," in *IEEE Transactions on Industrial Electronics*. Dec. 2018.
[35] F. Milano, "A Python-based Software Tool for Power System Analysis," IEEE PES General Meeting, Vancouver, Canada, 21-25 July 2013
[36] F. Milano, Power System Modelling and Scripting, Springer, London, August 2010.
[37] M. Howley and M. Holland, "Energy in Ireland 1990-2015, " Sustainable Energy Authority Of Ireland (SEAI), Nov. 2016.
[38] M. Khan, A. Milani, A. Chakrabortty, and I. Husain, "Dynamic Modeling and Feasibility Analysis of a Solid-State Transformer-Based Power Distribution System," IEEE Trans. Industry Applications, Vol. 54, No. 1, Jan/Feb. 2018.
[39] Y. Tu, J. Chen, H. Liu and T. O'Donnell, "Smart Transformer Modelling and Hardware in-the-loop Validation," *2019 IEEE 10th International Symposium on Power Electronics for Distributed Generation Systems (PEDG)*, Xi'an, China, 2019, pp. 1019-1025.
[40] Romero Navarro, Dynamic Load Models for Power Systems, 'Estimation of Time-Varying Parameters During Normal Operation', Lund university, Licentiate Thesis, Department of Industrial Electrical Engineering and Automation, 2002.